Title

Precious cargo: Modulation of the mesenteric lymph exosome payload after hemorrhagic shock.

Journal

The journal of trauma and acute care surgery, 86(1)

ISSN

2163-0755

Authors

Williams, Elliot C
Coimbra, Raul
Chan, Theresa W
et al.

Publication Date

2019

DOI

10.1097/ta.0000000000002093

Peer reviewed

Published in final edited form as:

J Trauma Acute Care Surg. 2019 January ; 86(1): 52–61. doi:10.1097/TA.0000000000002093.

Precious Cargo: Modulation of the Mesenteric Lymph Exosome Payload after Hemorrhagic Shock

Elliot C. Williams, MD[1], **Raul Coimbra, MD, PhD**[2], **Theresa W. Chan, MD**[1], **Andrew Baird, PhD**[1], **Brian P. Eliceiri, PhD**[1], **Todd W. Costantini, MD**[1]

[1]Division of Trauma, Surgical Critical Care, Burns and Acute Care Surgery, Department of Surgery, University of California San Diego Health. 200 W. Arbor Drive #8896, San Diego, CA, USA, 92103

[2]Riverside University Healthy System Medical Center, Loma Linda University School of Medicine, 26520 Cactus Ave, Moreno Valley, CA, USA 92555

BACKGROUND:

Trauma remains the leading cause of death up until the age of 45 in the United States, and the third leading cause of death overall (1). Despite advances in critical care, multiple organ failure (MOF) remains a significant contributor to late mortality after major trauma (2, 3). Patients who develop multiple organ failure have mortality rates varying from 27-100%, with mortality increasing for every additional organ involved (4). The model of post-injury multiple organ failure has advanced from early assumptions about overwhelming infection to recognition of a syndrome of hemorrhage and reperfusion injury followed by a dysregulated inflammatory response (5-7).

Since the 1950s, the gut has been proposed as a source for excessive inflammation and multiple organ failure after injury (8); however, it was not until the 1990s that Deitch et al. identified mesenteric lymph (ML) as a missing link connecting the gut and systemic inflammation. As such, ligating or diverting the mesenteric lymph ducts attenuates vascular permeability, decreases neutrophil priming, and prevents and acute lung injury (ALI) in models of trauma and hemorrhagic shock (T/HS), confirming the importance of the mesenteric lymph in mediating the systemic inflammatory response (9-12).

While mesenteric lymph has been implicated in multiple organ failure for two decades now, the specific mechanisms and the inflammatory mediators involved remain poorly defined. Previous studies have implicated that the lipid (13, 14), protein (15-17), and nucleic acid (18) components of mesenteric lymph are important in neutrophil priming and biological

Corresponding Author: Todd W. Costantini, MD, Division of Trauma, Surgical Critical Care, Burns and Acute Care Surgery, Department of Surgery, UC San Diego Health, 200 W. Arbor Drive #8896, San Diego, CA 92103, tcostantini@ucsd.edu.

AUTHOR CONTRIBUTIONS

E.C. Williams, R. Coimbra, T.W. Costantini, B.P. Eliceiri, and A. Baird designed research; E.C. Williams and T.W. Chan performed research and analyzed data. E.C. Williams wrote the manuscript with contributions from all authors. All authors reviewed and approved the final manuscript. This project was funded, in part, by a UC San Diego Academic Senate Health Sciences Research Grant (TWC).

Conflicts of interest: None

activity, and that they change after injury. To this end, our group has recently published data showing that exosomes, which are rich in lipids, proteins, and nucleic acids, are contained within the mesenteric lymph and are an important factor in driving inflammation and acute lung injury in a rodent T/HS model. Indeed, mesenteric lymph depleted of exosomes is devoid of detectable biological activity (19). Exosomes are nano-sized (30-150nm) extracellular vesicles that are actively secreted by most cell types and can be isolated from diverse bodily fluids, including blood, urine, cerebrospinal fluid, ascites, and lymph (20). Exosomes carry diverse payloads including proteins, lipids, mRNAs, and miRNAs, all of which may have biological activity and are capable of modulating the inflammatory response (21).

We have previously demonstrated that exosomes are present in rat ML, and that mesenteric lymph exosomes isolated after T/HS can trigger NF-κB activity and increase pro-inflammatory cytokine production in monocytes and macrophages (19) as well as causing dendritic cell (DC) dysfunction and apoptosis *in vitro* (22). More recently we showed that post-shock mesenteric lymph exosomes could replicate post-shock acute lung injury *in vivo* when injected into naïve animals, and that the activity of those exosomes was at least partially dependent on associated proteins (23); however, specific changes in the mesenteric lymph cargo after T/HS have not been identified.

While the exact mechanism of its effect has not been elucidated, stimulating the neuro-enteric axis via vagal nerve stimulation (VNS) is gut protective in multiple animal models of injury including burn (24) and traumatic brain injury (25) as well as T/HS; VNS has been shown to reduce gut barrier failure, decrease the pro-inflammatory activity of ML, and prevent post-shock acute lung injury (26-31). While we have previously shown that VNS alters the toxicity of the ML, its effect on mesenteric lymph exosomes is unknown.

In this study, we hypothesized that the gut ischemia/reperfusion associated with T/HS would lead to a distinct pro-inflammatory exosome phenotype in mesenteric lymph that could be identified by proteomic analysis with mass spectrometry (MS). With an eye towards therapeutic intervention, we further hypothesized that stimulating the neuro-enteric axis via vagal nerve stimulation would alter the proteomic profile of mesenteric lymph exosomes and decrease the biological activity of post-shock mesenteric lymph exosomes.

METHODS:

Animals

All experiments were carried out according to protocols approved by the Institutional Animal Care and Use Committee (IACUC) of the University of California, San Diego. Adult Male Sprague-Dawley rats weighing 300–350 grams were obtained from Harlan Laboratories (Harlan Sprague Dawley Inc., Placentia, CA). Animals were maintained in a temperature-controlled room (22 ± 2°C) on a 12-hour light/dark cycle, with access to standard food and water ad libitum throughout the study.

Trauma / Hemorrhagic Shock Model

Three animals per group were assigned to trauma with sham shock (T/SS), trauma with hemorrhagic shock (T/HS), and trauma with hemorrhagic shock and vagal nerve stimulation (T/HS + VNS). Animals were subjected to a model of T/HS as previously described (32). Briefly, animals were anesthetized with isoflurane (1-3%) and the left femoral artery and right jugular vein were cannulated with a polyethylene tube (PE-50). The mesenteric lymphatic duct was also cannulated with PE-50 tubing through midline laparotomy. Hemorrhagic shock was induced via withdrawal of blood from the jugular vein catheter until the mean arterial pressure was reduced to 35±5 mmHg and maintained for 60 minutes. At the end of the hemorrhagic shock, animals were resuscitated with shed blood plus two times shed blood volume in normal saline (Baxter, Deerfield, IL). For animals in the T/HS + VNS group, VNS was performed for the last 10 minutes of the hemorrhagic shock period using a square-wave generator at 5 V, with a frequency of 5 Hz as previously described (32). Trauma sham-shock (T/SS) animals underwent identical anesthesia and surgical procedures without hemorrhage. Mesenteric lymph was collected on ice during the pre-shock phase (60 minutes) and post-shock phase (60 minutes, starting 60 minutes after resuscitation), centrifuged at 2,000×g for 20 minutes to remove any cells and cellular debris, and stored at −80 °C until further analysis.

Isolation of exosomes from mesenteric lymph

Exosomes were isolated from ML using differential ultracentrifugation as described by Thery et al. (33). Briefly, ML samples were centrifuged first at 2,000g for 20 minutes to remove cells, then at 10,000g for 30 minutes to remove cellular debris and larger vesicles, and finally were subjected to ultracentrifugation at 100,000g for 70 minutes. The supernatant from this step was removed and stored at −80°C. The exosome pellets were washed and re-suspended in phosphate-buffered saline (PBS). Purified exosomes using this technique were characterized by electron microscopy, nanoparticle tracking analysis, and immunoblotting for CD63, CD81, and heat shock protein 70 as described in a previous study (19).

Nanoparticle Tracking Analysis

Exosome concentrations and size distribution profiles were obtained using a NanoSight NS300 instrument (Malvern Instruments, Malvern, UK) as previously detailed (19). Samples were recorded 3 times for 60 seconds using a camera level of 14, and NTA post-acquisition settings were optimized on a trial set then kept constant between samples. The concentration in particles per milliliter and size in nanometers was recorded for each sample.

Monocyte NF-κB Reporter Assay

Biological activity of exosomes was measured using THP1-Blue NF-κB cells (Invivogen, San Diego, CA) as previously described (19). Briefly, Cells were plated at 5 x10^5 cells/well in a 96 well plate and incubated with 10% (v/v) ML derived exosomes or their supernatant for 24 hours at 37 °C. After 24-hour incubation, 20ul of cell suspension was collected and incubated with 180μL of QUANTI-Blue (Invivogen) SEAP detection reagent for 4 hours at 37°C. SEAP activity was then assessed by a FLUOstar Omega spectrophotometric microplate reader (BMG Labtech, Ortenberg, Germany), using Omega software version

1.20, with absorbance read at 620nm wavelength. Experiments were performed in triplicate for three animals per group.

Liquid Chromatography Coupled with Tandem Mass Spectroscopy (LC-MS/MS)

Sample preparation: Exosome samples isolated from ML from the pre-shock and post-shock phases for two animals each in the T/HS and T/HS + VNS groups were equilibrated based on protein content and submitted to the Biomolecular and Proteomics Mass Spectrometry Facility (BPMSF) at UCSD for processing. Samples were diluted in TNE buffer (50mM Tris pH 8.0, 100mM NaCl, 1mM EDTA) and RapiGest SF surfactant (Waters Corp., Milford, MA) was added to the mix to a final concentration of 0.1% before samples were boiled for 5 minutes. TCEP (Tris (2-carboxyethyl) phosphine) was added to a 1mM final concentration and the samples were incubated at 37°C for 30 minutes. Samples were then carboxymethylated with 0.5 mg/ml of iodoacetamide for 30 minutes at 37°C then neutralized with TCEP at 2mM final concentration. Samples were then digested with trypsin (trypsin:protein ratio 1:50) overnight at 37°C. RapiGest was degraded and removed with 250mM HCl incubated at 37°C for 1 hour followed by centrifugation at 14,000g for 30 minutes at 4°C. The soluble fraction was then added to a new sterile tube and the peptides were extracted and desalted using C18 desalting columns (Thermo Scientific, PI-87782). Peptides were quantified using BCA assay and a total of 1ug of peptides were injected for LC-MS analysis.

LC-MS/MS: Trypsin-digested peptides prepared as above were analyzed by LC-MS/MS using nanospray ionization. The nanospray ionization experiments were performed using an Orbitrap fusion Lumos hybrid mass spectrometer (Thermo Fisher) interfaced with nano-scale reversed-phase ultra-high-pressure liquid chromatography (Dionex UltiMate™ 3000 RSLC nano System, Thermo Fisher) using a 25cm long, 75um internal diameter glass capillary packed with 1.7μm C18 (130) BEH™ beads (Waters corp.). Peptides were then eluted from the C18 column into the mass spectrometer using a linear gradient (5–80%) of Acetonitrile (ACN) at a flow rate of 375 μl/minute for 1 hour. The buffers used to create the ACN gradient were: Buffer A - 98% H_2O, 2% ACN, 0.1% formic acid, and Buffer B - 100% ACN, 0.1% formic acid. Mass spectrometer parameters were as follows: an MS1 survey scan using the Orbitrap detector (mass range (m/z): 400–1500 (using quadrupole isolation), 120,000 resolution setting, spray voltage of 2200 V, Ion transfer tube temperature of 275°C, AGC target of 400,000, and maximum injection time of 50 milliseconds), followed by data dependent scans (top speed for most intense ions, with charge state set to only include +2-5 ions, and 5 second exclusion time. While selecting ions with minimal intensities of 50,000 the collision event was carried out in the high energy collision cell (HCD collision energy of 30%), and the fragment masses were analyzed in the ion trap mass analyzer (ion trap scan rate of turbo, first mass m/z was 100, AGC Target 5000 and maximum injection time of 35 milliseconds).

Sequence Database Searches

PEAKS Studio 8.5 (Bioinformatics Solutions Inc., Waterloo, ON, Canada) was used for protein identification and label free quantification. PEAKS uses a database search and employs *de novo* sequencing as a subroutine to exploit the *de novo* sequencing results and

improve both the speed and accuracy of the database search. MS/MS data was searched against the Rat Swissprot database with the following search parameters: Parent Mass Error Tolerance: 15.0ppm, Fragment Mass Error Tolerance: 0.5Da, Precursor Mass Search Type: monoisotopic, Enzyme: Trypsin, Max Missed Cleavages: 3, Non-specific Cleavage: one, Max Variable PTM Per Peptide: 3, De novo score (ALC%) threshold: 15, Peptide hit threshold (−10logP): 30.0. A modified target decoy approach is then used to determine the minimum peptide spectrum matching score threshold to meet the FDR requirement (set here at 1.5%). Highly differentially expressed proteins between pre-shock and post-shock groups were established by PEAKS en-suite statistical analysis tool (fold change >2, FDR < 0.01, Unique tryptic peptides ≥ 2). All uncharacterized proteins were excluded from analysis. Proteomic data is reported here using published reporting guidelines (34), and more detail on the PEAKS algorithms is available (35).

Statistics

Protein abundance data calculated by PEAKS Studio analysis was subjected to additional criteria for final protein selection. Any spectra below the significance threshold set by the PEAKS studio software were eliminated, as well as proteins found in only one of the two biological replicates. Differences in relative abundance from pre-shock to post-shock were calculated individually for each animal, using the pre-shock condition as an internal control to account for variability between animals. Paired 2-sample t-tests were performed and P values were adjusted for multiple testing using Benjamini and Hochberg's procedure (36), setting the expected proportion of false discoveries to 0.05. Because this study was hypothesis generating, the multiple-comparison adjusted P value was accepted as $P < 0.1$, however only proteins with individual P values <0.05 and adjusted P value < 0.1 were considered significant.

All non-proteomic data was compared using one-way ANOVA followed by post-hoc Tukey's HSD test to compare individual means and $P < 0.05$ was considered significant.

Bioinformatics

All validated unique proteins as well as subgroups of proteins with significant differences in abundance between groups were analyzed for functional enrichments and Gene Ontology (GO) pathways (37) using the freely available STRING database (https://string-db.org/). Proteins that were determined to be significantly different in the initial PEAKS Studio analysis were entered into the Ingenuity Pathway Analysis (IPA) software (Qiagen, Redwood City, CA). The "core analysis" function was used to interpret the differentially expressed data, including, biological processes and canonical pathways. Right-tailed Fisher's exact test was used to calculate the probability that each biological function and/or disease assigned to that network is due to chance alone. Morpheus matrix visualization and analysis software was used to create heatmaps (https://software.broadinstitute.org/morpheus).

RESULTS:

T/HS ML Exosome Proteomics

After application of validation criteria outlined above, an aggregated 287 unique proteins expressed by ML exosomes remained for analysis. GO analysis of all proteins showed significant enrichment in the “extracellular region” (147 proteins, FDR = $9x10^{-70}$) and “extracellular exosome” (90 proteins, FDR = $9x10^{-42}$) cellular components. Eight proteins were found to be unique to post-shock exosomes and were not identified in the pre-shock group (Table 1). PEAKS studio identified 110 of these proteins as changing significantly after T/HS. The complete protein list is available as Supplementary Digital Content 1. After statistical analysis of relative protein abundance, 35 proteins were significantly increased in the post-shock phase compared to pre-shock (Table 2). Twenty-two of these proteins have been shown to be increased in prior proteomic studies analyzing whole, unfractionated ML after T/HS, while 15 are identified for the first time in this study (17, 38, 39). There were no proteins significantly decreased in the post-shock phase.

Quantification and Sizing of Exosomes Isolated from ML after T/HS or T/HS + VNS by NTA

The concentration of exosomes in the ML was significantly decreased during the post-shock phase compared to pre-shock in both the T/HS ($1.70x10^{10} \pm 1.07x10^{9}$ vs. $1.2x10^{10} \pm 7.3x10^{8}$, $p<0.01$) and T/HS + VNS ($1.66x10^{10} \pm 5.34x10^{8}$ vs. $1.18x10^{10} \pm 5.59x10^{8}$, $p<0.01$) groups. These were also significantly decreased compared to SS ($1.51x10^{10} \pm 7.29x10^{8}$, both $p<0.01$). There was no difference between SS and either of the pre-shock groups (Fig 1A). These results are consistent with our previous findings of decreased concentrations of exosomes in post-resuscitation ML (19). The average size of ML exosomes did not change during any of the time points or conditions as shown in Figure 1B.

Effect of VNS on ML Exosome Protein Content

An aggregated total of 170 proteins met the identification validity standards, and of these 134 overlapped with those identified in the T/HS group. The 8 proteins previously found only in the post-shock lymph were not detected in the pre-shock or post-shock samples in the VNS group. Only one protein was significantly increased in the post-shock T/HS + VNS group compared to pre-shock, GAPDH (17-fold increase, $p < 0.01$, corrected $p < 0.05$). A heat map comparing the most significant proteomic changes between the T/HS group and the T/HS + VNS groups demonstrates that VNS alters the protein phenotype of ML exosomes with expression patterns similar to pre-shock (Figure 2). The complete T/HS + VNS protein list is available as Supplementary Digital Content 2.

Bioinformatics Analysis of T/HS and T/HS + VNS Proteomics Changes

Using IPA we explored the relationships between all proteins that met validity criteria and were identified by PEAKS Studio as having differential expression between pre-shock and post-shock phases for either group (96 from T/HS group and 32 from T/HS + VNS group). This allowed us to determine the canonical pathways and disease/functional networks involved in post-hemorrhagic shock exosomes from the ML. The most significant of these are presented in Figure 3.

VNS Modulation of Biological Activity of Exosomes from ML

The biological activity of both ML exosomes and the supernatant from which they were isolated was evaluated using an *in vitro* human monocyte NF-κB reporter assay. T/SS ML exosomes were compared to post-shock T/HS and T/HS + VNS ML exosomes. There was a significant increase in induction of NF-κB activity after exposure to post-shock T/HS exosomes compared to exposure to ML exosomes from T/SS or supernatant. Conversely, post-shock exosomes from the T/HS + VNS group did not alter monocyte NF-κB activity (Fig. 4). These findings demonstrate that activation of the neuro-enteric axis via vagal nerve stimulation is able to directly alter the inflammatory activity of exosomes from the gut after T/HS.

DISCUSSION:

The results presented here represent the first description of the proteomics of exosomes isolated from mesenteric lymph after trauma and hemorrhagic shock. Post-shock mesenteric lymph exosomes carry a distinct phenotypic protein cargo that includes novel proteins as well as proteins seen in previous studies evaluating whole, unfractionated mesenteric lymph (17, 38, 39). This protein phenotype shows enrichment in pathways for cell death and survival, organismal injury, and the inflammatory response among others. Further, we demonstrate that stimulating the vagus nerve prevents the T/HS-induced changes in mesenteric lymph exosome protein payload, and suggests a novel mechanism by which the neuro-enteric axis may limit the systemic inflammatory response after injury.

Previous studies evaluating the systemic inflammatory response to injury have proposed that the release of tissue-toxic factors into the mesenteric lymphatic system was a “missing link” between ischemia/reperfusion injury of the gut and remote organ injury (12). Current models describing the “gut-lymph” hypothesis (40) propose that after major injury and gut hypoperfusion there is a disturbance in the integrity of the gut-barrier and an increase in intestinal permeability, allowing endotoxin or other injurious factors to cross the epithelial barrier. The gut inflammatory response leads to the production of toxic factors and danger-associated molecular patterns (DAMPs) which are carried through the mesenteric lymphatics and reach the systemic circulation. Although a significant body of research has focused on identifying the specific injurious factors responsible for, and the molecular mechanisms behind this connection, the exact nature of these factors remains to be identified. Previous studies have appeared conflicting, in that they proscribed activity to different fractions of whole lymph, such as lipid (13, 14), protein (15-17), and nucleic acid (18) components.

Our group recently identified exosomes within the mesenteric lymph as important carriers of danger signals from the gut (19), which can unify previous results thought to be discordant because exosomes are rich in all of these diverse cargo molecules. Further, we have shown that d exosome-depleted lymph is not biologically active which suggests that these other potential inflammatory mediators are not floating free in the lymph (19). Growing evidence supports the role of exosomes in cell to cell communication, and have shown exosome payloads to be major mediators of inflammation in a diverse array of pathologies including pancreatitis, atherosclerosis, chronic kidney disease, and sepsis (41-45). We previously demonstrated that post-shock mesenteric lymph exosomes are able to cause acute lung

injury in naïve mice *in vivo* and activate alveolar macrophages via a TLR4-dependent mechanism *in vitro* (23). Exosomes carry a diverse cargo: proteins, lipids, mRNAs, and miRNAs; and which of these are the biologically active factors carried in the mesenteric lymph exosomes after trauma and major injury remains uncertain. In our most recent study we also noted that treating post-shock exosomes with a proteinase decreased, but did not completely abolish their ability to stimulate TNF-α production in macrophages, implying that exosome surface proteins may be involved (23). Here, we demonstrated that proteins carried by exosomes in mesenteric lymph are altered after T/HS, creating a pro-inflammatory protein phenotype that may lead to a diagnostic or therapeutic target.

There is considerable interest in discovering translatable interventions to limit the systemic inflammatory response and multi-organ failure after T/HS. Multiple groups have published the protective effect of stimulating the neuro-enteric axis either electrically via vagal nerve stimulation or pharmacologically via vagal agonists (30, 31). Indeed, we have shown in multiple injury models that VNS prevents intestinal barrier dysfunction, decreases the biological activity of post-shock ML, and prevents acute lung injury after major trauma (24, 27, 28, 46, 47). We predicted that VNS performed after T/HS would abrogate the changes in mesenteric lymph exosomes previously seen in the post-shock phase. While VNS did not change the size of exosomes after T/HS nor did it prevent the decrease in concentration of exosomes in the post-shock phase, we found dramatic changes in the mesenteric lymph exosome protein payload in VNS treated animals compared to T/HS alone. Only one protein increased a statistically significant amount in the VNS group compared to 35 in the T/HS post-shock exosomes, and bioinformatics analysis of these proteins showed that VNS decreased the expression of proteins associated with inflammation and injury. We subsequently found that post-shock mesenteric lymph exosomes from the T/HS group induced significant production of NF-κB from a monocyte cell line, whereas post-shock T/HS + VNS exosomes were similar to T/SS and did not induce the monocyte NF-κB inflammatory response. A chain of exosome cross-talk has been described from intestinal epithelial cells to mucosal dendritic cells which can then traffic to mesenteric lymph nodes and interact with T-cells prior to release into the mesenteric lymph ducts (48). Activation of the neuro-enteric axis may have direct effects at multiple points in this pathway. Previous studies have shown that vagal nerve stimulation reduces gut epithelial cell damage by activating intestinal glial cells in a burn injury model (24), but also that vagal nerve stimulation can modulate $CD103^{+}$ dendritic cell trafficking to the mesenteric lymph nodes (32), providing multiple potential mechanisms for modulation of exosome production by vagal nerve stimulation.

In summary, we demonstrate that exosomes released by the gut into mesenteric lymph after T/HS have a distinctive proteome that is enriched for proteins involved in injury and inflammatory pathways, consistent with their ability to induce inflammation i*n vitro* and cause acute lung injury *in vivo*. We also show that stimulation of the vagal nerve prevents the development of this pro-inflammatory exosome phenotype both in terms of protein content and in biological activity. This study is limited by a small sample size in our proteomic samples, which likely reduced the number of significant changes in proteins and may have caused underestimation of protein changes. Further studies are needed to verify which specific protein or proteins are critical to the inflammatory activity of mesenteric

lymph exosomes and confirm changes seen in proteomics. Additionally, protease addition only partially reduced inflammatory activity of post-shock exosomes, and thus it is worthwhile to examine the role of other exosome cargo, including nucleic acids like mRNA, microRNA, and DNA. Future studies characterizing the mechanism regulating toxic exosome released into the mesenteric lymph after injury are critical to defining potential therapeutic targets to limit SIRS.

Supplementary Material

Refer to Web version on PubMed Central for supplementary material.

ACKNOWLEDGMENTS

We thank Dr. Majid Ghassemian (BPMSF, University of California, San Diego) for his support with the LC-MS/MS, Dr. Antonio De Maio (Department of Surgery, University of California, San Diego) for his support with the Nanoparticle Tracking Analysis, and Dr. Mitsuaki Kojima (Trauma and Acute Critical Care Medical Center, Tokyo Medical and Dental University) for his support with animal surgical techniques. The authors declare no conflicts of interest.

REFERENCES

1. Heron M Deaths: Leading Causes for 2016. Natioinal Vital Statistics Reports. 2016;67(6):1–77.
2. Benns M, Carr B, Kallan MJ, Sims CA. Benchmarking the incidence of organ failure after injury at trauma centers and nontrauma centers in the United States. J Trauma Acute Care Surg. 2013;75(3):426–31. [PubMed: 24089112]
3. Durham RM, Moran JJ, Mazuski JE, Shapiro MJ, Baue AE, Flint LM. Multiple organ failure in trauma patients. J Trauma. 2003;55(4):608–16. [PubMed: 14566110]
4. Lee CC, Marill KA, Carter WA, Crupi RS. A current concept of trauma-induced multiorgan failure. Ann Emerg Med. 2001;38(2):170–6. [PubMed: 11468613]
5. Schweinburg FB, Seligman AM, Fine J. Transmural migration of intestinal bacteria; a study based on the use of radioactive Escherichia coli. N Engl J Med. 1950;242(19):747–51. [PubMed: 15412704]
6. Faist E, Baue AE, Dittmer H, Heberer G. Multiple organ failure in polytrauma patients. J Trauma. 1983;23(9):775–87. [PubMed: 6620431]
7. Fry DE, Pearlstein L, Fulton RL, Polk HC Jr. Multiple system organ failure. The role of uncontrolled infection. Arch Surg. 1980;115(2):136–40. [PubMed: 6965449]
8. Waydhas C, Nast-Kolb D, Jochum M, Trupka A, Lenk S, Fritz H, Duswald KH, Schweiberer L. Inflammatory mediators, infection, sepsis, and multiple organ failure after severe trauma. Arch Surg. 1992;127(4):460–7. [PubMed: 1348412]
9. Adams CA Jr., Hauser CJ, Adams JM, Fekete Z, Xu DZ, Sambol JT, Deitch EA. Trauma-hemorrhage-induced neutrophil priming is prevented by mesenteric lymph duct ligation. Shock. 2002;18(6):513–7. [PubMed: 12462558]
10. Deitch EA, Adams C, Lu Q, Xu DZ. A time course study of the protective effect of mesenteric lymph duct ligation on hemorrhagic shock-induced pulmonary injury and the toxic effects of lymph from shocked rats on endothelial cell monolayer permeability. Surgery. 2001;129(1):39–47. [PubMed: 11150032]
11. Deitch EA, Adams CA, Lu Q, Xu DZ. Mesenteric lymph from rats subjected to trauma-hemorrhagic shock are injurious to rat pulmonary microvascular endothelial cells as well as human umbilical vein endothelial cells. Shock. 2001;16(4):290–3. [PubMed: 11580112]
12. Magnotti LJ, Upperman JS, Xu DZ, Lu Q, Deitch EA. Gut-derived mesenteric lymph but not portal blood increases endothelial cell permeability and promotes lung injury after hemorrhagic shock. Ann Surg. 1998;228(4):518–27. [PubMed: 9790341]

13. Gonzalez RJ, Moore EE, Biffl WL, Ciesla DJ, Silliman CC. The lipid fraction of post-hemorrhagic shock mesenteric lymph (PHSML) inhibits neutrophil apoptosis and enhances cytotoxic potential. Shock. 2000;14(3):404–8. [PubMed: 11028564]

14. Gonzalez RJ, Moore EE, Ciesla DJ, Biffl WL, Offner PJ, Silliman CC. Phospholipase A(2)--derived neutral lipids from posthemorrhagic shock mesenteric lymph prime the neutrophil oxidative burst. Surgery. 2001;130(2):198–203. [PubMed: 11490349]

15. Jordan JR, Moore EE, Sarin EL, Damle SS, Kashuk SB, Silliman CC, Banerjee A. Arachidonic acid in postshock mesenteric lymph induces pulmonary synthesis of leukotriene B4. J Appl Physiol (1985). 2008;104(4):1161–6. [PubMed: 18276905]

16. Dayal SD, Hauser CJ, Feketeova E, Fekete Z, Adams JM, Lu Q, Xu DZ, Zaets S, Deitch EA. Shock mesenteric lymph-induced rat polymorphonuclear neutrophil activation and endothelial cell injury is mediated by aqueous factors. J Trauma. 2002;52(6):1048–55; discussion 55. [PubMed: 12045629]

17. D'Alessandro A, Dzieciatkowska M, Peltz ED, Moore EE, Jordan JR, Silliman CC, Banerjee A, Hansen KC. Dynamic changes in rat mesenteric lymph proteins following trauma using label-free mass spectrometry. Shock. 2014;42(6):509–17. [PubMed: 25243424]

18. Blenkiron C, Askelund KJ, Shanbhag ST, Chakraborty M, Petrov MS, Delahunt B, Windsor JA, Phillips AR. MicroRNAs in mesenteric lymph and plasma during acute pancreatitis. Ann Surg. 2014;260(2):341–7. [PubMed: 24509209]

19. Kojima M, Gimenes-Junior JA, Langness S, Morishita K, Lavoie-Gagne O, Eliceiri B, Costantini TW, Coimbra R. Exosomes, not protein or lipids, in mesenteric lymph activate inflammation: Unlocking the mystery of post-shock multiple organ failure. J Trauma Acute Care Surg. 2017;82(1):42–50. [PubMed: 27779585]

20. Colombo M, Raposo G, Thery C. Biogenesis, secretion, and intercellular interactions of exosomes and other extracellular vesicles. Annu Rev Cell Dev Biol. 2014;30:255–89. [PubMed: 25288114]

21. Raposo G, Stoorvogel W. Extracellular vesicles: exosomes, microvesicles, and friends. J Cell Biol. 2013;200(4):373–83. [PubMed: 23420871]

22. Kojima M, Costantini TW, Eliceiri BP, Chan TW, Baird A, Coimbra R. Gut epithelial cell-derived exosomes trigger posttrauma immune dysfunction. J Trauma Acute Care Surg. 2018;84(2):257–64. [PubMed: 29194317]

23. Kojima M, Gimenes-Junior JA, Chan TW, Eliceiri BP, Baird A, Costantini TW, Coimbra R. Exosomes in postshock mesenteric lymph are key mediators of acute lung injury triggering the macrophage activation via Toll-like receptor 4. FASEB J. 2018;32(1):97–110. [PubMed: 28855278]

24. Costantini TW, Bansal V, Krzyzaniak M, Putnam JG, Peterson CY, Loomis WH, Wolf P, Baird A, Eliceiri BP, Coimbra R. Vagal nerve stimulation protects against burn-induced intestinal injury through activation of enteric glia cells. Am J Physiol Gastrointest Liver Physiol. 2010;299(6):G1308–18. [PubMed: 20705905]

25. Bansal V, Costantini T, Ryu SY, Peterson C, Loomis W, Putnam J, Elicieri B, Baird A, Coimbra R. Stimulating the central nervous system to prevent intestinal dysfunction after traumatic brain injury. J Trauma. 2010;68(5):1059–64. [PubMed: 20453760]

26. Levy G, Fishman JE, Xu D, Chandler BT, Feketova E, Dong W, Qin Y, Alli V, Ulloa L, Deitch EA. Parasympathetic stimulation via the vagus nerve prevents systemic organ dysfunction by abrogating gut injury and lymph toxicity in trauma and hemorrhagic shock. Shock. 2013;39(1):39–44. [PubMed: 23247120]

27. Langness S, Costantini TW, Morishita K, Eliceiri BP, Coimbra R. Modulating the Biologic Activity of Mesenteric Lymph after Traumatic Shock Decreases Systemic Inflammation and End Organ Injury. PLoS One. 2016;11(12):e0168322. [PubMed: 27977787]

28. Morishita K, Coimbra R, Langness S, Eliceiri BP, Costantini TW. Neuroenteric axis modulates the balance of regulatory T cells and T-helper 17 cells in the mesenteric lymph node following trauma/hemorrhagic shock. Am J Physiol Gastrointest Liver Physiol. 2015;309(3):G202–8. [PubMed: 26045612]

29. Morishita K, Costantini TW, Ueno A, Bansal V, Eliceiri B, Coimbra R. A pharmacologic approach to vagal nerve stimulation prevents mesenteric lymph toxicity after hemorrhagic shock. J Trauma Acute Care Surg. 2015;78(1):52–8; discussion 8-9. [PubMed: 25539203]
30. Levy G, Fishman JE, Xu DZ, Dong W, Palange D, Vida G, Mohr A, Ulloa L, Deitch EA. Vagal nerve stimulation modulates gut injury and lung permeability in trauma-hemorrhagic shock. J Trauma Acute Care Surg. 2012;73(2):338–42; discussion 42. [PubMed: 22846937]
31. Li JG, Hu ZF, Du ZH, Zhou Q, Jia BH, Peng ZQ, Ye XF, Li B. [Protective effect of the cholinergic anti-inflammatory pathway against hemorrhagic shock in rats]. Zhongguo Wei Zhong Bing Ji Jiu Yi Xue. 2005;17(1):24–7. [PubMed: 15636707]
32. Morishita K, Costantini TW, Eliceiri B, Bansal V, Coimbra R. Vagal nerve stimulation modulates the dendritic cell profile in posthemorrhagic shock mesenteric lymph. J Trauma Acute Care Surg. 2014;76(3):610–7; discussion 7-8. [PubMed: 24553526]
33. Thery C, Amigorena S, Raposo G, Clayton A. Isolation and characterization of exosomes from cell culture supernatants and biological fluids. Curr Protoc Cell Biol. 2006;Chapter 3:Unit 3 22.
34. Latterich M Publishing proteomic data. Proteome Sci. 2006;4:8. [PubMed: 16643670]
35. Zhang J, Xin L, Shan B, Chen W, Xie M, Yuen D, Zhang W, Zhang Z, Lajoie GA, Ma B. PEAKS DB: de novo sequencing assisted database search for sensitive and accurate peptide identification. Mol Cell Proteomics. 2012;11(4):M111 010587.
36. Green GH, Diggle PJ. On the operational characteristics of the Benjamini and Hochberg False Discovery Rate procedure. Stat Appl Genet Mol Biol. 2007;6:Article27.
37. Ashburner M, Ball CA, Blake JA, Botstein D, Butler H, Cherry JM, Davis AP, Dolinski K, Dwight SS, Eppig JT, et al. Gene ontology: tool for the unification of biology. The Gene Ontology Consortium. Nat Genet. 2000;25(1):25–9. [PubMed: 10802651]
38. Mittal A, Middleditch M, Ruggiero K, Loveday B, Delahunt B, Jullig M, Cooper GJ, Windsor JA, Phillips AR. Changes in the mesenteric lymph proteome induced by hemorrhagic shock. Shock. 2010;34(2):140–9. [PubMed: 20160674]
39. Peltz ED, Moore EE, Zurawel AA, Jordan JR, Damle SS, Redzic JS, Masuno T, Eun J, Hansen KC, Banerjee A. Proteome and system ontology of hemorrhagic shock: exploring early constitutive changes in postshock mesenteric lymph. Surgery. 2009;146(2):347–57. [PubMed: 19628095]
40. Assimakopoulos SF, Triantos C, Thomopoulos K, Fligou F, Maroulis I, Marangos M, Gogos CA. Gut-origin sepsis in the critically ill patient: pathophysiology and treatment. Infection. 2018.
41. Bonjoch L, Casas V, Carrascal M, Closa D. Involvement of exosomes in lung inflammation associated with experimental acute pancreatitis. J Pathol. 2016;240(2):235–45. [PubMed: 27447723]
42. Carney EF. Chronic kidney disease: Key role of exosomes in albumin-induced inflammation. Nat Rev Nephrol. 2018;14(3):142.
43. Gao W, Liu H, Yuan J, Wu C, Huang D, Ma Y, Zhu J, Ma L, Guo J, Shi H, et al. Exosomes derived from mature dendritic cells increase endothelial inflammation and atherosclerosis via membrane TNF-alpha mediated NF-kappaB pathway. J Cell Mol Med. 2016;20(12):2318–27. [PubMed: 27515767]
44. Roig-Arcos J, Lopez-Malo D, Diaz-Llopis M, Romero FJ. Exosomes derived from stimulated monocytes promote endothelial dysfunction and inflammation in vitro. Ann Transl Med. 2017;5(12):258. [PubMed: 28706926]
45. Essandoh K, Yang L, Wang X, Huang W, Qin D, Hao J, Wang Y, Zingarelli B, Peng T, Fan GC. Blockade of exosome generation with GW4869 dampens the sepsis-induced inflammation and cardiac dysfunction. Biochim Biophys Acta. 2015;1852(11):2362–71. [PubMed: 26300484]
46. Bansal V, Costantini T, Kroll L, Peterson C, Loomis W, Eliceiri B, Baird A, Wolf P, Coimbra R. Traumatic brain injury and intestinal dysfunction: uncovering the neuro-enteric axis. J Neurotrauma. 2009;26(8):1353–9. [PubMed: 19344293]
47. Costantini TW, Bansal V, Peterson CY, Loomis WH, Putnam JG, Rankin F, Wolf P, Eliceiri BP, Baird A, Coimbra R. Efferent vagal nerve stimulation attenuates gut barrier injury after burn: modulation of intestinal occludin expression. J Trauma. 2010;68(6):1349–54; discussion 54-6. [PubMed: 20539179]

48. Smythies LE, Smythies JR. Exosomes in the gut. Front Immunol. 2014;5:104. [PubMed: 24672525]

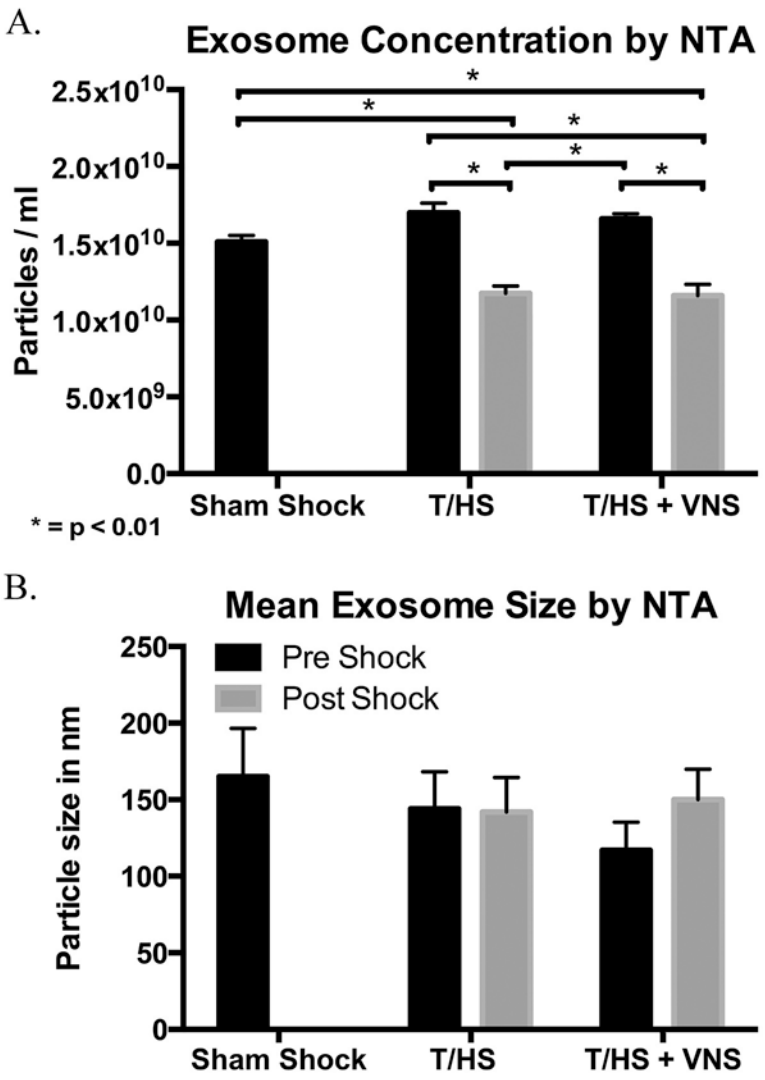

Figure 1. Concentration and mean size of ML exosomes.

Vagal nerve stimulation (VNS) does not affect the size or concentration of exosomes in mesenteric lymph (ML) after trauma/hemorrhagic shock (T/HS). Exosomes isolated from ML from T/SS animals vs. the pre-shock (grey) or post-shock (black) phase after either T/HS or T/HS with VNS. Analyzed by NanoSight NS300 and expressed as mean +/− SE, N=3 for each group. (A) Mean size of exosomes from ML is not significantly different in any group or condition. (B) Mean concentration of exosomes (particles/ml) is lower in the post-shock phase for both T/HS and T/HS + VNS groups (*p<0.05).

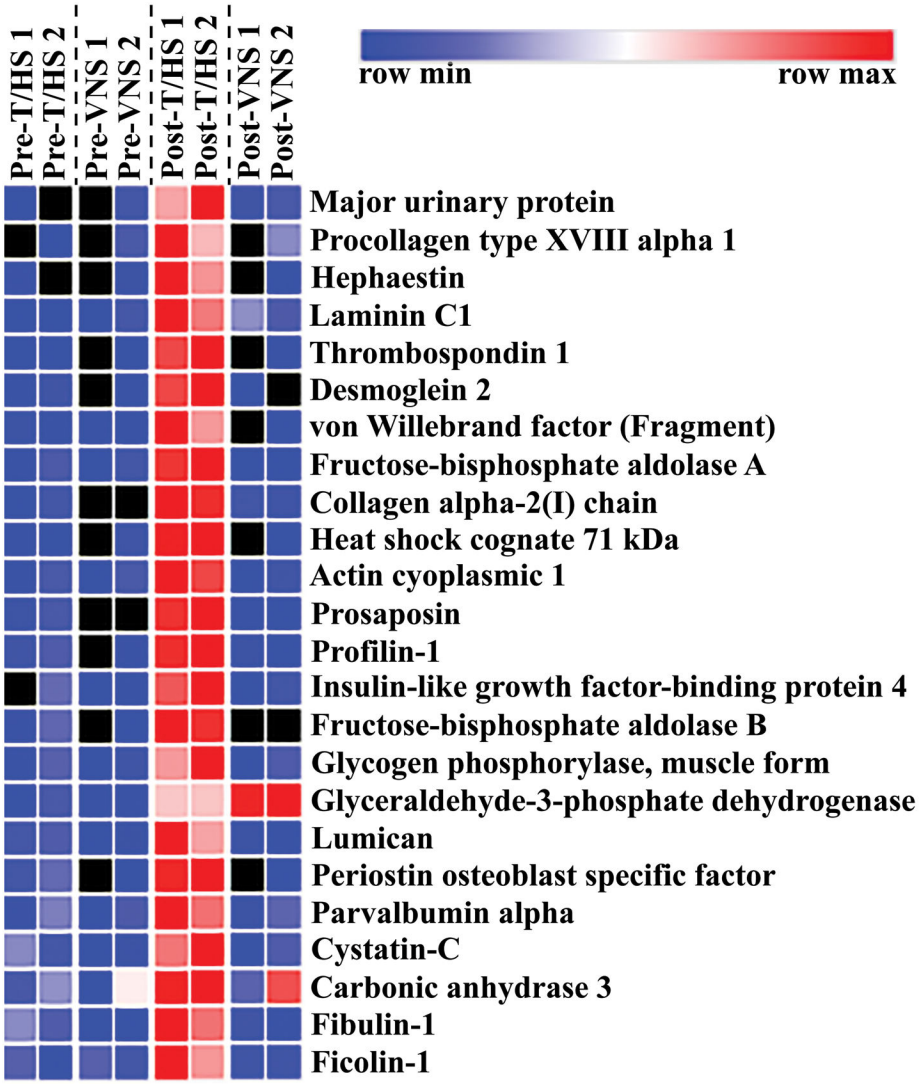

Figure 2. Heat map of protein expression changes after T/HS or T/HS with VNS.

Vagal nerve stimulation (VNS) after trauma/hemorrhagic shock (T/HS) mitigates the post-shock proteomic phenotype. Values increase progressively from blue to red in the color scale, with black values representing protein not identified or below threshold of detection. Proteins were quantified by a label free quantitative proteomics approach on paired samples (pre-shock and post-shock) from N=2 for each of T/HS and T/HS + VNS groups. Protein identification and label free quantification was carried out using PEAKS Studio 8.5 (Bioinformatics Solutions Inc.). Quantitative values were used for heat mapping with the software Morpheus (https://software.broadinstitute.org/morpheus).

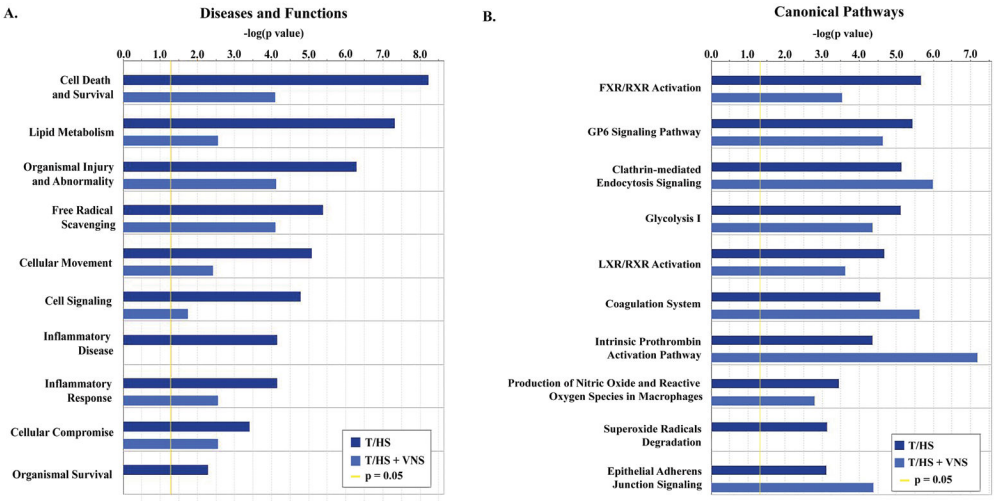

Figure 3. Ingenuity Pathway Analysis (IPA) gene ontology analysis of proteins increased in post-shock phases of T/HS or T/HS with VNS.

Protein identification and label free quantification was carried out using PEAKS Studio 8.5 (Bioinformatics Solutions Inc.), with N=2 per condition. Post-shock values were compared to pre-shock for each group and all proteins with ≥2 unique peptides and determined to be significantly increased were entered into the IPA software and a comparison analysis performed between T/HS and T/HS + VNS groups. For both (A) Top Diseases and Functions and (B) Canonical Pathways the graph shows enrichment in pathways as represented by −log (p value) from Fisher's exact test, with a threshold set here of 1.3 (p = 0.05).

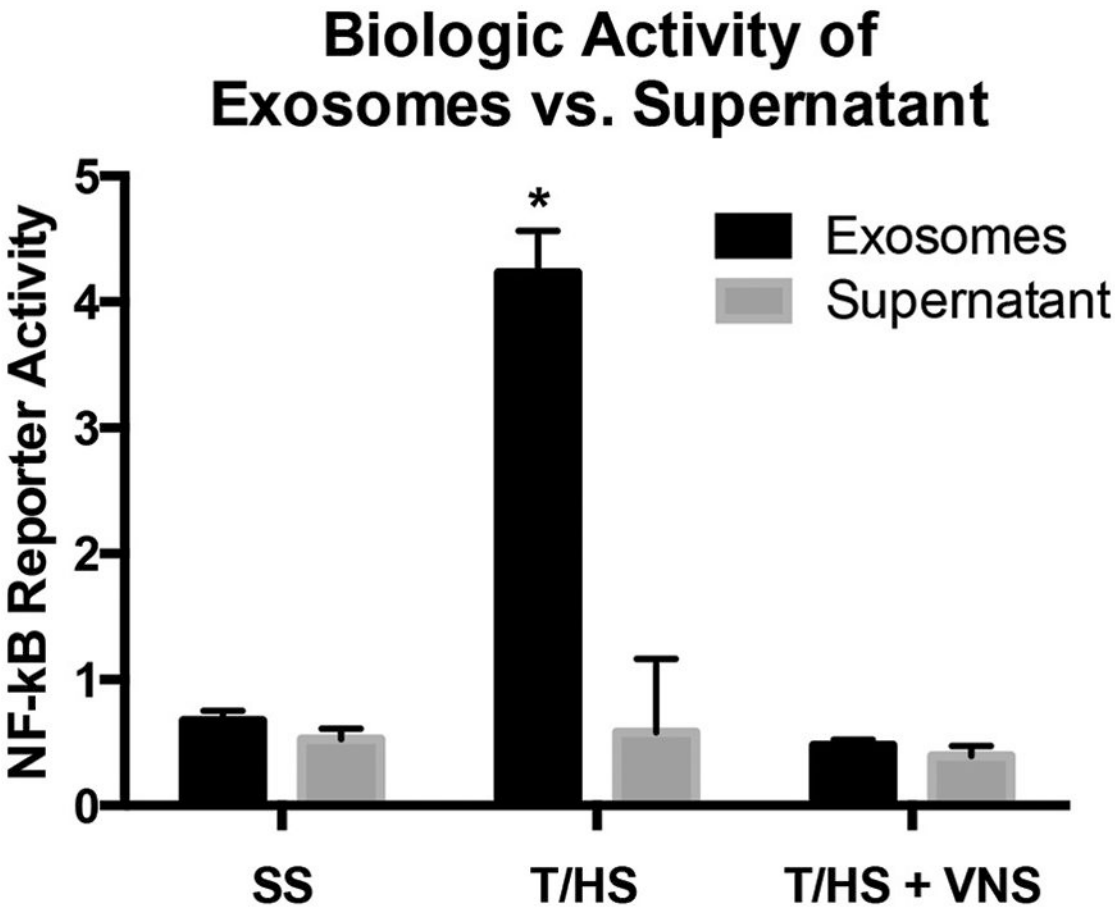

Figure 4. Activation of an NF-kB reporter by ML exosomes or supernatant in a monocytic cell line model.

Effect of VNS on biological activity of ML exosomes. THP-1 Blue NF-κB reporter monocytes were stimulated with 10% v/v re-suspended exosomes (black) or supernatant (grey) isolated from ML during the post-shock phase of the T/HS and T/HS + VNS models and compared to ML from T/SS animals. OD compared to standard curve of LPS and results expressed as mean +/− SD of 3 animals per group. *p<0.001 versus all other groups.

TABLE 1.

Identification of Mesenteric Lymph Exosome Proteins Unique to the Post-Shock Phase After Trauma/ Hemorrhagic Shock

Protein Name	Gene Symbol	UniProt ID	Location	Molecular Function
Decorin	Dcn	Q01129	Extracellular matrix	Collagen binding
Signal peptide, CUB domain and EGF-like domain containing 1	Scube1	F1M987	Plasma membrane	Calcium ion binding
Chymotrypsin-like	Ctrl	G3V8J3	Extracellular region	Serine-type endopeptidase activity
Phospholipase B1, membrane-associated	Plb1	O54728	Apical cell membrane	phospholipase A2 activity
Exostosin glycosyltransferase 1	Ext1	G3V901	Endoplasmic reticulum	Protein homo/hetero dimerization
Serine peptidase inhibitor, Kunitz type 1	Spint1	Q4V8Q2	Plasma membrane	serine-type endopeptidase inhibitor
WD repeat-containing protein 1	Wdr1	Q5RKI0	Cytoskeleton	Actin filament binding
Renin Receptor	Atp6ap2	Q6AXS4	Plasma membrane	Enzyme binding

TABLE 2.

Proteins Significantly Increased in Post-Shock Mesenteric Lymph Exosomes Compared to Pre-Shock

Protein	UniProt ID	Fold Increase	*p* Value	Adjusted *p* Value	
Major urinary protein	P02761	78.2	0.035	0.062	*a,c*
Procollagen type XVIII alpha 1	F1LR02	55.7	0.045	0.076	
Hephaestin	Q920H8	41.7	0.029	0.045	*a*
Laminin C1	F1MAA7	39.0	0.018	0.045	
Thrombospondin 1	A0A0G2JV24	26.4	0.100	0.045	
Cofilin-1	P45592	21.4	0.031	0.071	*a,b*
Coronin-1A	Q91ZN1	20.0	0.010	0.032	
Desmoglein 2	F1LYX9	18.0	0.006	0.020	*b*
von Willebrand factor (Fragment)	Q62935	15.5	0.033	0.062	
Ribonuclease 4	O55004	15.1	0.006	0.026	*a*
Thymosin beta-4	P62329	14.9	0.011	0.005	*a*
Fructose-bisphosphate aldolase A	P05065	14.2	0.006	0.005	*a,b*
Collagen alpha-2(I) chain	P02466	13.0	0.003	0.020	
Heat shock cognate 71 kDa	P63018	12.9	<0.001	0.005	*a,b*
Actin, cytoplasmic 1	P60711	11.3	0.008	0.031	*a,b,c*
Prosaposin	P10960	10.8	0.003	0.005	*a*
Profilin-1	P62963	9.4	0.003	0.005	*a,b*
Desmocolin 2	D3ZJR7	9.1	0.016	0.045	
Insulin-like growth factor-binding protein 4	P21744	8.6	0.027	0.020	*a*
Fructose-bisphosphate aldolase B	P00884	8.1	0.011	0.035	*a,b*
Glycogen phosphorylase, muscle form	P09812	7.7	0.046	0.031	*a,b*
72 kDa type IV collagenase	P33436	7.6	0.029	0.020	*a*
L-lactate dehydrogenase A chain	P04642	7.5	0.026	0.062	*a,b*
Lysozyme C-1	P00697	7.1	0.021	0.031	*a,b*
Glyceraldehyde-3-phosphate dehydrogenase	MOR660	7.0	0.009	0.026	*a*
Lumican	P51886	6.7	0.047	0.076	*a,b*
Periostin osteoblast specific factor	D3ZAF5	6.3	0.007	0.020	
Procollagen C-endopeptidase enhancer 1	O08628	6.2	0.004	0.020	
Urinary protein 1-like	D3ZIF6	6.2	0.005	0.020	
Parvalbumin alpha	P02625	6.1	0.042	0.076	*a,c*
Fibulin-5	Q9WVH8	5.2	0.004	0.020	
Cystatin-C	P14841	4.6	0.043	0.077	*a,b*

Protein	UniProt ID	Fold Increase	*p* Value	Adjusted *p* Value	
Carbonic anhydrase 3	P14141	4.0	0.014	0.026	*a,b,c*
Fibulin-1	D3ZQ25	3.4	0.037	0.020	
Ficolin-1	Q9WTS8	3.2	0.045	0.026	

a = Also increased in D'Allesandro et al Shock 2014; 42(6): 509–517

b = Also increased in Mittal et al Shock 2010; 32(2):140-9

c = Also increased in Peltz et al Surgery 2009; 146(2):347-57